In Situ Imaging and Height Reconstruction of Phase Separation Processes in Polymer Blends during Spin Coating

Stephen Ebbens,[†,*] Richard Hodgkinson,[†] Andrew J. Parnell,[‡] Alan Dunbar,[†] Simon J. Martin,[§] Paul D. Topham,[⊥] Nigel Clarke,[‡] and Jonathan R. Howse[†,*]

[†]Department of Chemical and Biological Engineering, The University of Sheffield, Sheffield. S1 3JD. U.K., [‡]Department of Physics and Astronomy, The University of Sheffield, Sheffield, S3 7RF. U.K., [§]Department of Materials, Loughborough University, Loughborough, LE11 3TU, U.K., and [⊥]Department of Chemical Engineering and Applied Chemistry, Aston University, Birmingham, B4 7ET, U.K.

ABSTRACT Spin coating polymer blend thin films provides a method to produce multiphase functional layers of high uniformity covering large surface areas. Applications for such layers include photovoltaics and light-emitting diodes where performance relies upon the nanoscale phase separation morphology of the spun film. Furthermore, at micrometer scales, phase separation provides a route to produce self-organized structures for templating applications. Understanding the factors that determine the final phase-separated morphology in these systems is consequently an important goal. However, it has to date proved problematic to fully test theoretical models for phase separation during spin coating, due to the high spin speeds, which has limited the spatial resolution of experimental data obtained during the coating process. Without this fundamental understanding, production of optimized micro- and nanoscale structures is hampered. Here, we have employed synchronized stroboscopic illumination together with the high light gathering sensitivity of an electron-multiplying charge-coupled device camera to optically observe structure evolution in such blends during spin coating. Furthermore the use of monochromatic illumination has allowed interference reconstruction of three-dimensional topographies of the spin-coated film as it dries and phase separates with nanometer precision. We have used this new method to directly observe the phase separation process during spinning for a polymer blend (PS—PI) for the first time, providing new insights into the spin-coating process and opening up a route to understand and control phase separation structures.

KEYWORDS: polymer blends · spin coating · microscope · photovoltaic cells

There has been a long-standing interest in developing an understanding of the processes occurring during the spin coating of multiphase polymeric materials from a common solvent. This interest has originated in part from the potential applications of the rich variety of morphologies generated, such as the ability to serve as self-organized patterned substrates with regular micrometer-scale features.[1] This attention has recently intensified due to the additional attraction of using organic materials within electronic devices, for example in photovoltaic devices where the nanoscale phase separation determines device efficiency.[2] Motivated by these real-world applications, understanding phase separation during spin coating has consequently been a subject of theoretical interest[3] and has established a challenging benchmark for models of polymer phase phenomena.[4] Spin-coating phase-separated morphologies result from a liquid—liquid phase transition occurring as the common solvent for both components evaporates and a subsequent liquid to solid transition, either through crystallization or vitrification. These processes and thus final film morphologies have been experimentally shown to depend on a wide range of factors including features of the individual polymers (molecular weight,[5] solubility,[6] surface tension, viscosity), the blended solution (solid content,[7] solvent properties,[6] blend ratio[8]), and the substrate (chemistry,[6] roughness, size, shape) along with details of the coating process such as spin speed,[1] acceleration, and atmosphere.[9] Based on the assembled experimental data a wide range of models have been proposed to account for the reported parametric relationships that rely on assumptions about the dynamic behavior during spin coating such as vertical solvent gradients,[3] Marangoni instabilities, and stratification.[10] However, to date, verifying and assessing these dynamic phenomena experimentally has been limited by the available characterization tools, which have crucially been unable to directly capture spatially resolved information during the coating process.

During the spin-coating process the horizontal substrate is rotated at speeds between

* Address correspondence to j.r.howse@sheffield.ac.uk.

Received for review March 31, 2011 and accepted May 11, 2011.

Published online May 11, 2011
10.1021/nn201210e

1000 and 10 000 rpm, limiting attempts to perform direct imaging during coating to low spatial resolution analysis applicable only for macroscopic phenomena.[11,12] As a result of the limited spatial resolution of these high-speed photography methods, morphological studies of phase separation in thin film polymer blends, which generally occurs on the micrometer and nanoscale, have relied upon static optical microscopy and scanning probe microscopy of the final frozen morphology,[6] in some cases combined with inferred morphology development from laser reflectance measurements,[7] a method originally outlined by Hass *et al.*[13] As an example, Jukes *et al.*[14] demonstrated the ability to use off-specular laser scattering signal to provide information about the evolution of in-plane length scales during film formation. In these laser methods it is also possible to simultaneously use fluctuations in reflected intensity to back-calculate spatially averaged drying rate curves for the area illuminated by the laser using Bragg's law (constructive interference occurs when 2nd cos $\theta_i = m\lambda$, where n = refractive index of the film, d is the thickness, θ_i is the angle of incidence relative to the normal, and λ is the wavelength).[15−17] For example, Heriot *et al.* used modeling of this specular signal intensity together with the off-specular scattering pattern to infer that for a blend of poly(styrene) and poly(methylmethacrylate) the phase separation process was driven by Marangoni effect disruption of stratified layers.[10] More recently Mokarian-Tabari *et al.* used the same technique to investigate the effects of solvent atmosphere for directing the final morphology as well as investigating the effect of radial sheer upon phase separation by offsetting the incident laser relative to the center of rotation.[9]

This approach has the benefit of high temporal resolution for the reflected signal due to the high intensity of the laser, but suffers as the development of in-plane structure has to be inferred from the scattering data by converting from reciprocal space into real space and then matched to the final morphology. Moreover, the scattering data collected are spatially averaged by sample rotation, due to the limited speed of data capture and exposure time for the CCD camera, and obtained from a sample area limited by the laser footprint (typically a few mm). This reliance on an indirect estimate of the spatial evolution of final structure has hampered the goal of fully characterizing spin-coating phase separation processes and thus developing robust theories that can in turn be used to improve and control the performance of the resulting functional and regularly structured materials.

In this study we have used a direct imaging approach and exploited improved optics, light sources, and video capture methods to demonstrate a straightforward method to allow micrometer-scale lateral resolution and nanometer vertical precision metrology during the spin-coating phase separation of a polymer blend from solution, paving the way to the fundamental insights needed to develop the highly controlled spin-coating morphologies required for the next generation of advanced materials.

To achieve this, we have synchronously triggered a short pulse from a high-power, narrow-bandwidth, green LED (520 nm, $\Delta\lambda$ 10 nm) and a high-sensitivity electron-multiplier charge-coupled device camera connected to a conventional episcopic optical microscope to record a series of stroboscopically frozen images of the rotating spin-coating substrate, with one frame captured every full revolution. This has been achieved with sufficient precision to repeatedly image the same region of the spinning disk with an error less than the optical limit throughout the duration of the coating process. The duration of the pulse (50 μs) is sufficiently short that a 400 μm field of view, near the center of rotation, appears static at spin speeds up to 3000 rpm. To generate a better understanding of the processes involved in the phase separation of polymer blends, we have directed our studies toward a blend of high molecular weight polystyrene (PS) (MW = 577.5 k) and poly(isoprene) (PI) (MW 800 k) dissolved in a low vapor pressure solvent (*o*-xylene), spun at 1500 rpm and so consequently imaged at 25 fps. The high molecular weights of the polymers and the relatively low vapor pressure of *o*-xylene ensure the length scales are clearly optically visible and that the phase separation and drying are relatively slow. This blend is also remarkable for the reproducibility and uniformity of the final morphology, providing a robust system to demonstrate this method.[8,18]

RESULTS AND DISCUSSION

Typical stroboscopically illuminated images captured during spin-coating deposition of a PS:PI blend onto a silicon substrate at 1500 rpm are shown in Figure 1. It is apparent that the optical image quality is high, with no evidence of motion blur, even at the edges of the images, showing the short LED pulse length has produced the desired frozen images. In addition, the lateral position of features in the image series remains consistent, showing that the triggering procedure has ensured illumination of the same region of the spinning sample with high precision. As a result, with the experimental setup described above, it is now possible to directly observe the evolution of microstructure during polymer blend spin coating with a clarity and resolution similar to that obtained from conventional optical microscopy of a static sample. The movie from which Figure 1 shows extracts is available as Supporting Information.

As the illumination was chosen to have a narrow bandwidth to allow interferometric height reconstruction, the contrast in the stroboscopic images shown in Figure 1 is primarily due to constructive and destructive interference between reflections at the air−solution

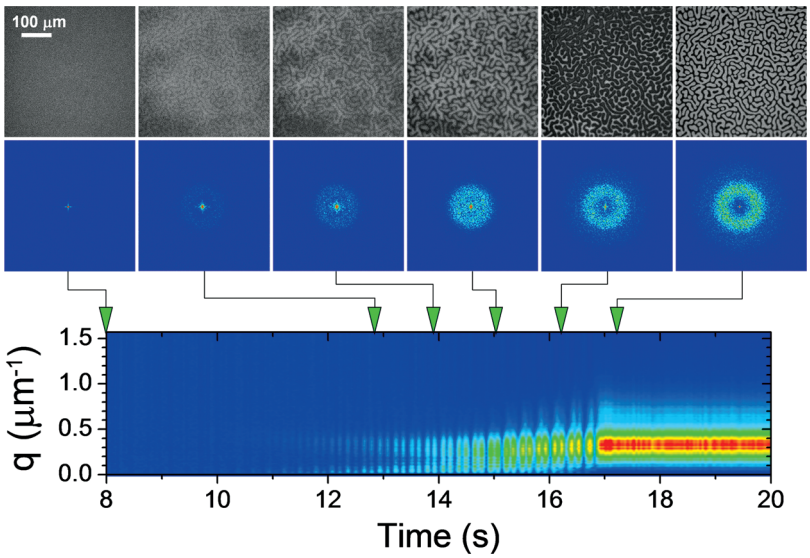

Figure 1. At the top a series of unprocessed stroboscopic optical reflectance images recorded during spin coating of a 1:1 blend of PS:PI (2% wt at 1500 rpm) from *o*-xylene are shown. The images were illuminated with narrow-bandwidth green light at the indicated times during the spin-coating process (taken from Movie 1 Supporting Information). Corresponding background-corrected 2D Fourier transforms are shown underneath each frame, with the radial integral of the Fourier transform for the entire movie shown below.

interface and the solution–silicon interface. Consequently the image contrast reflects the instantaneous height differences at the sample surface. Due to the similar refractive index of the two polymers and the solvent, very little additional optical contrast is expected. As the absolute height of the film is also constantly reducing due to solvent evaporation/material ejection, periodic interference contrast inversions occur according to Bragg's law, for example as seen between the last two still frames, Figure 1.[19] With this interpretation it is apparent that as the solution is initially spun, we have a flat uniform sample surface (0–12 s, see video) evident from the uniform intensity. From approximately 12 seconds onward, it is possible to determine weak, large-scale fluctuations of approximately 100 μm in length, which are increasingly dominated by shorter length scale domain features (approximately 20 μm) with positions that appear to remain fixed with time right through the coating process to the final dried state (17.2 s). This reflects the expected stages of the spin-coating process. Initially solvent concentration is high enough for the blend components to remain miscible;[20] however after a certain amount of time sufficient shear and evaporative thinning has occurred to commence the liquid–liquid phase transition to an immiscible solution (around 12.8 s here), followed by further solvent loss to reach the eventual final dry film morphology. This final morphology is consistent with the bicontinuous phase separation reported for similar PS:PI blends at 1:1 ratios.[18]

From the radially integrated Fourier transformed data we can follow the evolution of the two length scales during the coating process. The longer length scale decreases in length as the film dries, converging with the length scale corresponding to the obvious phase separation domain structure. It is interesting to note that, of the two length scales present, it is that of the phase separation that dominates the final lateral structure. This length scale agrees with the mean phase-separated phase domain size in the final real-space optical image and shows a phase-separated length scale of ~18 μm (q = 0.35 μm^{-1}), which is consistent throughout the phase separation process. The 2D Fourier transforms show the isotropic nature of both length scales.

The images and FFT analysis consequently indicate that the final phase-separated structure evolves very little after the liquid–liquid transition occurs, despite solvent evaporation continuing for a further 5 s. The larger length scale structure is likely to be due to weak Marangoni instabilities due to solvent evaporation. However in this case these instabilities have little influence on the final structure. This ability to directly observe the development of phase separation and Marangoni phenomena in this way provides a valuable new method to explore in more detail proposals made about the extent to which they inter-relate in a range of systems.

Due to the interference phenomena that determine the intensity of the reflected optical signal, analysis of the oscillations in intensity at each image pixel as a function of time allows the corresponding drying rate of the film to be determined and mapped across the entire field of view, in analogy to existing interference microscopy techniques and the spatially averaged specular laser methods discussed above. The former topographical reconstruction methods require as a

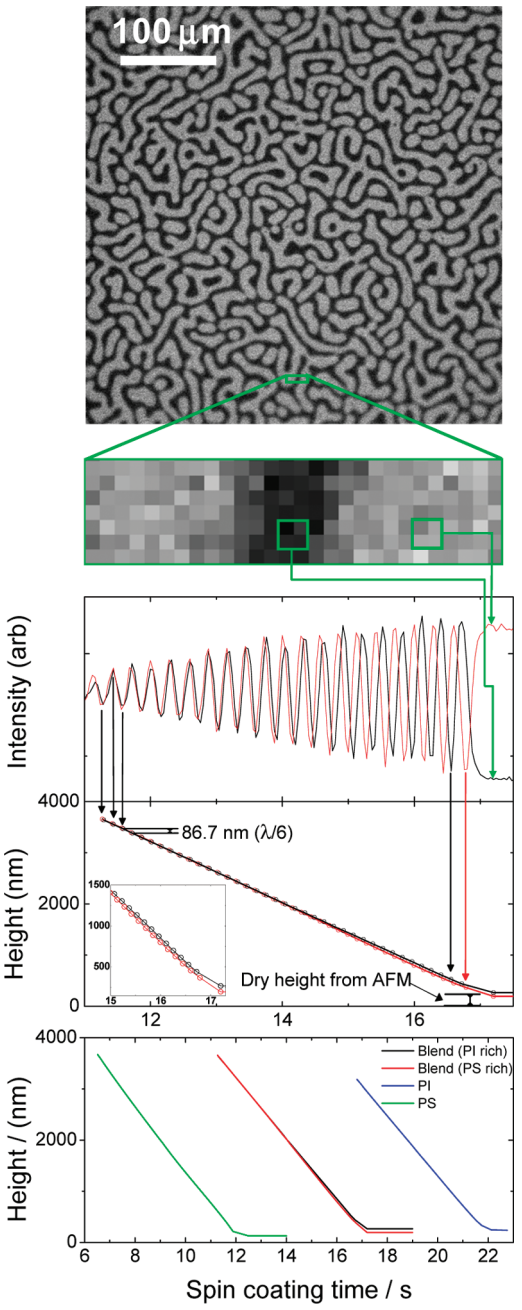

Figure 2. Process used to extract quantitative drying curves from stroboscopic interference image time stacks. The optical image sequence is used to generate intensity *versus* time graphs for each pixel position across the field of view. The top graph shows example curves for representative final "bright" and "dark" 2 × 2 pixel binned regions. Maxima and minima peak position times are used to reconstruct corresponding spatially resolved drying curves (middle graph, inset shows detail of the final drying stage). Lower graph shows the drying curves for typical blend domains compared to homopolymer samples at the same wt %, with final thickness determined by ellipsometry.

reference point either a known position of the reference beam in the case of spatial modulation or through a known surface when fringe counting.[21] In our case we instead use the assumption of flat uniform film morphology at a sufficiently early stage of film formation as a starting point.[22] The way this approach is applied to produce an array of drying curves with high spatial resolution is illustrated in Figure 2. From the overlay of typical reflected intensity curves it is apparent that at the start of the reconstruction (<12 s, Figure 2) the interference intensities are in phase, consistent with the assumption of a flat uniform starting morphology. However, as the spin-coating process continues, a phase shift develops, due to the appearance of topographical differences (12−15 s). We consequently apply an automated fringe counting algorithm from this reference point onward to produce drying curves for each pixel location across the image. These drying curves are then placed on an absolute height scale by adjusting their mean end height to correspond to estimates of average final sample thickness obtained by AFM scratch testing and ellipsometry (see Supporting Information). Typical drying curves reveal that there is a consistent difference in the drying rate between the optically "bright" and "dark" domains, which results in the predicted height difference between these locations in the final morphology, such that optically dark domains actually dry more slowly and to a higher final position. Comparison with the same analysis applied for equivalent homopolymer samples (Figure 2, bottom) shows that pure PS dries completely within 12 s of spin coating, whereas PI takes 22 s to dry. The blend dry film end point lies at the midpoint between these values. In addition, the drying rate over the final 6 s reconstructed is faster for PS than PI, and ellipsometry indicates that the final PS film thickness is less than that for PI. This would suggest that optically "bright", lower lying, faster drying domains are PS rich, and the surrounding optically "dark" higher domains are PI rich. Selective washing has confirmed this assignment, showing that drying curve determination in this way can allow material identification.

Because this approach can be applied at every pixel across our optical images, it is possible to extend this method to reconstruct by interpolation the absolute quantitative sample height across the entire field of view at any stage during the drying process, as shown in Figure 3.

The validity of the assumption of uniform film morphology with low roughness at the start time chosen for the drying curve reconstruction and the approach in general can be tested by comparing the final reconstructed morphology with AFM metrology carried out at the same region of the final sample surface, Figure 4. This comparison reveals excellent agreement with lateral structures in the reconstruction matching those seen in the AFM image down to the optical limit. Cross-section analysis reveals quantitative agreement between the reconstructed and "real" AFM data in the *z*-direction within 10% accuracy. In addition, comparison of histograms of the reconstruction

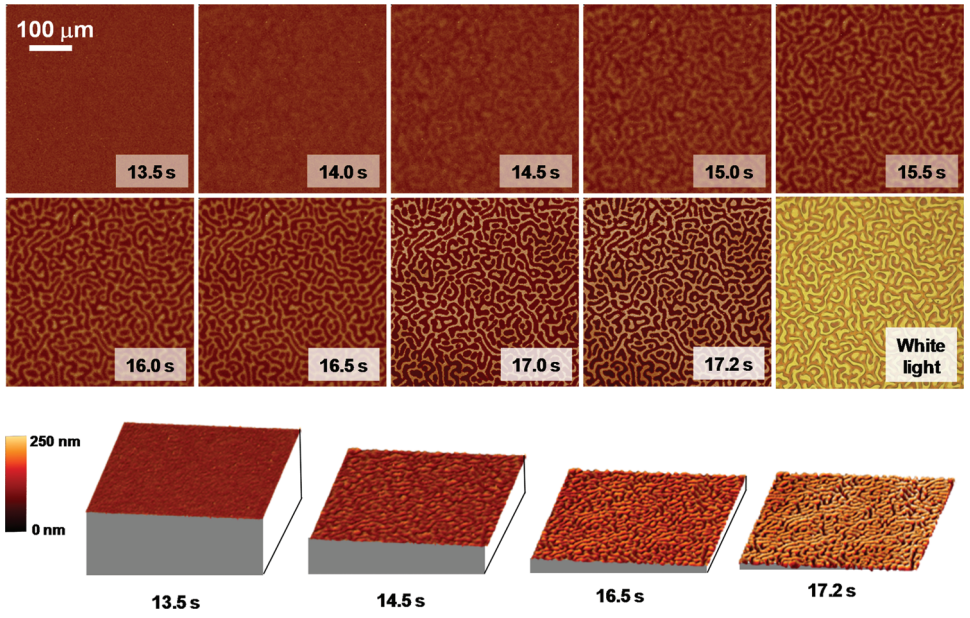

Figure 3. (Top) 2D relative height reconstructions during spin coating a PS:PI blend at 1500 rpm obtained from pixel by pixel drying curve arrays generated from fringe counting the stroboscopic optical images. (Bottom) 3D surface morphology reconstructions.

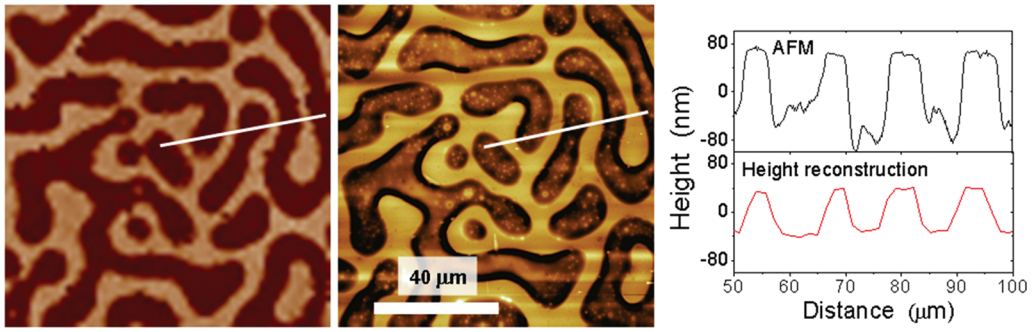

Figure 4. Comparison of detail and a virtual cross section of the final optically reconstructed morphology (left) with AFM phase imaging morphology (middle) and section (right).

reveals an average height difference between the high and low domains of 70 nm compared to 91 nm for similar analysis of the AFM image. In this way we verify the ability of this narrow bandwidth stroboscopic illumination and reconstruction approach to quantitatively visualize the evolution of phase-separating surface morphology with high spatial resolution on a rapidly rotating disk. It is further noted that the error of the sample height will be greatest in the final morphology, due to the cumulative additive nature of the drying curve reconstruction, and height reconstructions earlier in the drying process will have increased fidelity to the true morphology. This excellent morphological agreement also allows conventional AFM to be used to assess any later ongoing morphological development that may occur as the sample ages.

The final morphology shown in Figure 4 consists of two distinct domains separated by a consistent height step, with a bicontinuous structure, corresponding to the contrast in an optical image of the same location. In the reconstruction, and more clearly in the AFM morphology data, it can be seen that there are also smaller length scale circular domain structures (diameter 100–1000 nm) that appear sunken within the high domains or raised within the low domains. This suggests small inclusions of the neighboring phase were trapped during the larger domain structure formation and underwent a secondary localized phase separation process at some stage during drying. As discussed above, the bicontinuous phase-separated morphology appears well before the drying process is complete and does not undergo significant lateral translation after t his point. This is illustrated further in Figure 5. Here features that appear in the final surface topography are initially visible in the reconstructed topography at a stage in the drying process when the film thickness is greater than 2 μm, around 10 times the final dried film thickness. Indeed, FFT analysis of the raw optical images indicates that features at this length scale are first visible around 11 s after spin

coating begins, a full 6 s before the sample dries, Figure 1. This early surface structure supports the previous theoretical prediction that phase separation originates at the surface first and that this original structure forms a motif to direct the subsequent phase separation of solvent richer underlying regions.[3] These morphological reconstructions also confirm the suggestions above, that phase separation in the PI–PS system appears to follow a straightforward spinodal decomposition process, with little influence of the Marangoni instabilities that appear in early optical images.

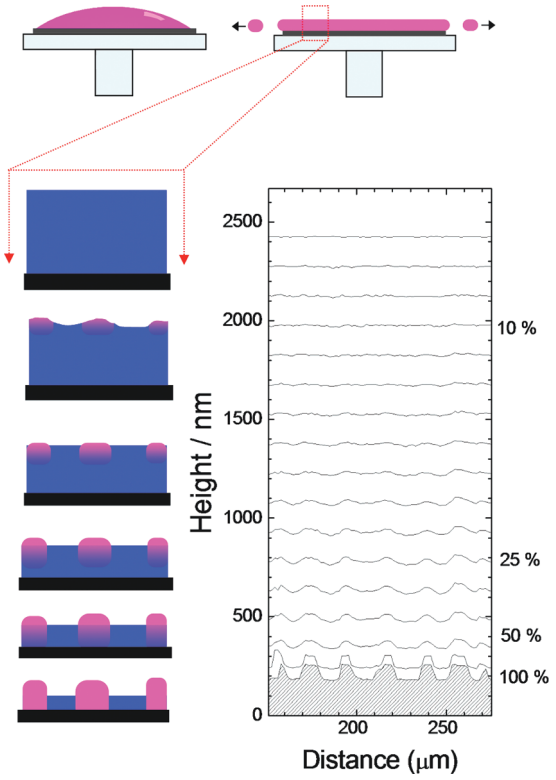

Figure 5. (Left) Schematic cross section during the phase separation process. (Right) Quantitative reconstructed surface topography at 0.25 s intervals (start time 13 s). Estimated polymer content labeled on right-hand axis.

Despite the relatively fixed nature of the overall bicontinuous structure during the last several seconds of drying, fine details of the phase-separated morphology appear to develop over the last fraction of seconds of the drying process. In Figure 6, necks can be seen to develop between adjacent sunken domains. In addition, fine-scale features, which correspond to the circular inclusions in the final morphology discussed above, are seen to develop. This indicates that this secondary phase separation occurs as the remaining small amount of solvent evaporates from the blend. At this stage diffusion lengths are significantly reduced, preventing phase material from adopting the primary separation motif.

CONCLUSION

In summary, we have demonstrated a powerful narrow-bandwidth illumination stroboscopic microscopy method to allow high-quality optical micrographs to be obtained throughout the spin-coating procedure and accurate absolute height reconstruction for the final part of the drying process, with comparable vertical resolution to AFM micrographs. We have used this method to confirm that the phase-separation process in 1:1 PS–PI blends is dominated by spinodal

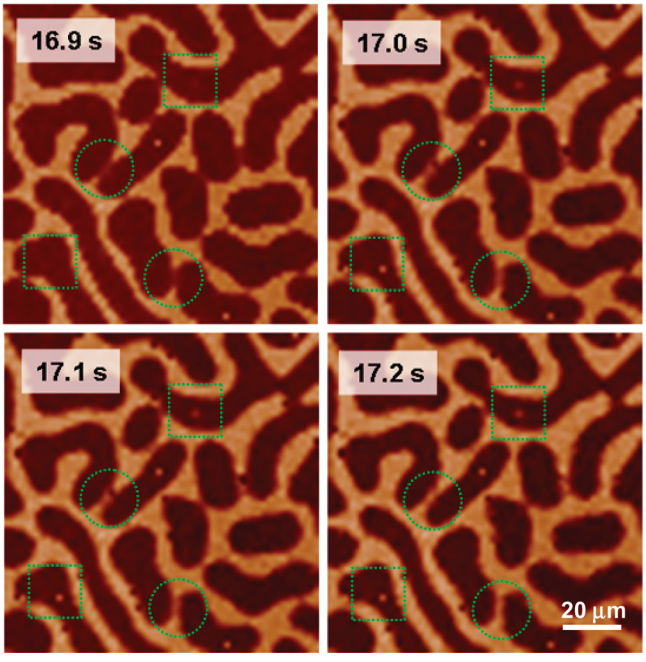

Figure 6. Evolution of fine structure during the final stage of film formation. Circles show necking behavior; squares show small-scale phase separation.

decomposition, resulting in the appearance of bicontinuous morphology that originates around 4 s before the film has completely dried. This surface motif roughens as the film dries; however little further lateral evolution occurs at this length scale. This is consistent with the model developed by Buxton *et al.*,[3] which predicts initial phase separation occurring at the top surface of the nascent film where the solvent concentration is lowest, followed by development of this motif as the underlying material phase separates. During the final fraction of a second we see evidence for a secondary phase separation process, again consistent with the diffusion limit placed on the final solvent evaporation. In addition, a larger scale surface roughness early in the spin-coating process is assigned to Marangoni instabilities, but in this system has little influence on the final morphology and phase structure.

Increasing the understanding of the interplay between phase separation and Marangoni effects for polymer blends spun cast from solution using this new method and gathering direct evidence for the early development of surface phase separation can in turn produce improved theoretical understanding and control of functional morphologies for polymer blend based devices. It should also be noted that comparable high-resolution visualization of the dynamics of phase separation for thin polymer blends undergoing phase separation at elevated temperatures has previously been achieved using atomic force microscopy on static samples.[23] However direct comparison for the data we report here with these studies is difficult due to the complication of the third solvent phase present during spin coating and the resulting dynamic increase in polymer weight percent that occurs during phase separation.

EXPERIMENTAL SECTION

Polymer blends of PI and PS were prepared by dissolving the homopolymers in *o*-xylene (Sigma Aldrich, >99%) at 2% wt, followed by filtration (Whatman PTFE filter at 0.45 μm) and blending in a 1:1 ratio by volume. A square of freshly oxygen plasma cleaned silicon wafer (10 mm $\times$ 10 mm) was placed upon a rotating disk attached to a dc motor, mounted under a 20$\times$ microscope objective (Nikon), and 20 μL of the polymer blend was dispensed onto the surface and then spun at 1500 rpm. Illumination from a 100 W green LED (λ_{center} = 520 nm, width 10 nm) was focused on the surface using the episcopic optics of the microscope. A custom-built electronic trigger connected to the motor commutators fired the LED with a pulse duration of 50 μs once every revolution and simultaneously triggered image capture. The short duration of the individual pulse, and use of monochromatic light, limited the photon flux available for microscopy and therefore required a fast, high-sensitivity camera, in this instance an EMCCD with a quantum efficiency of ~95% (ANDOR, iXon 897). Typically movies were recorded as 16-bit TIFF stacks, for ~30 s at 25 fps, as defined by the motor spin speed. In our experimental geometry the Bragg equation for constructive interference simplifies to $d = m\lambda/3$ (approximating both polymer and solvent refractive indices to $n = 1.5$). Using monochromatic illumination at 520 nm, this gave consecutive constructive interference occurring every time the film thins by 173.33 nm. It should be noted that, due to the finite width of the illumination, the amplitude of the interference effect decays as the film thickness increases (*i.e.*, at earlier, more solvent-rich periods during the spin-coating process). This produced the enveloping of the intensity oscillations shown in Figure 2. Image analysis and height reconstruction were performed using Labview software, and three-dimension topographies were rendered using Povray. AFM micrographs were captured with a Veeco Explorer microscope operating in tapping mode.

Acknowledgment. J.R.H. acknowledges the EPSRC (EP/G04077X/1).

Supporting Information Available: Videos obtained during the spin-coating process and the corresponding FFT are available free of charge via the Internet at http://pubs.acs.org.

REFERENCES AND NOTES

1. Fang, L. A.; Wei, M.; Barry, C.; Mead, J. Effect of Spin Speed and Solution Concentration on the Directed Assembly of Polymer Blends. *Macromolecules* **2010**, *43*, 9747–9753.
2. He, X. M.; Gao, F.; Tu, G. L.; Hasko, D.; Huttner, S.; Steiner, U.; Greenham, N. C.; Friend, R. H.; Huck, W. T. S. Formation of Nanopatterned Polymer Blends in Photovoltaic Devices. *Nano Lett.* **2010**, *10*, 1302–1307.
3. Buxton, G. A.; Clarke, N. Ordering Polymer Blend Morphologies Via Solvent Evaporation. *EPL* **2007**, 78.
4. Souche, M.; Clarke, N. Phase Equilibria in Polymer Blend Thin Films: A Hamiltonian Approach. *J. Chem. Phys.* 2009, *131*, 244903.
5. Li, X.; Xing, R. B.; Zhang, Y.; Han, Y. C.; An, L. J. Molecular Weight Effects on the Phase Morphology of PS/P4VP Blend Films on Homogeneous SAM and Heterogeneous SAM/Au Substrates. *Polymer* **2004**, *45*, 1637–1646.
6. Walheim, S.; Boltau, M.; Mlynek, J.; Krausch, G.; Steiner, U. Structure Formation Via Polymer Demixing in Spin-Cast Films. *Macromolecules* **1997**, *30*, 4995–5003.
7. Dunbar, A. D. F.; Mokarian-Tabari, P.; Parnell, A. J.; Martin, S. J.; Skoda, M. W. A.; Jones, R. A. L. A Solution Concentration Dependent Transition from Self-Stratification to Lateral Phase Separation in Spin-Cast Ps:D-Pmma Thin Films. *Eur. Phys. J. E* **2010**, *31*, 369–375.
8. DalnokiVeress, K.; Forrest, J. A.; Stevens, J. R.; Dutcher, J. R. Phase Separation Morphology of Thin Films of Polystyrene/Polyisoprene Blends. *J. Polym. Sci., Polym. Phys.* **1996**, *34*, 3017–3024.
9. Mokarian-Tabari, P.; Geoghegan, M.; Howse, J. R.; Heriot, S. Y.; Thompson, R. L.; Jones, R. A. L. Quantitative Evaluation of Evaporation Rate During Spin-Coating of Polymer Blend Films: Control of Film Structure through Defined-Atmosphere Solvent-Casting. *Eur. Phys. J. E* **2010**, *33*, 283–289.
10. Heriot, S. Y.; Jones, R. A. L. An Interfacial Instability in a Transient Wetting Layer Leads to Lateral Phase Separation in Thin Spin-Cast Polymer-Blend Films. *Nat. Mater.* **2005**, *4*, 782–786.
11. Melo, F.; Joanny, J. F.; Fauve, S. Fingering Instability of Spinning Drops. *Phys. Rev. Lett.* **1989**, *63*, 1958–1961.
12. Birnie, D. P.; Haas, D. E.; Hernandez, C. M. Laser Interferometric Calibration for Real-Time Video Color Interpretation of Thin Fluid Layers During Spin Coating. *Opt. Laser Eng.* *48*, 533−537.
13. Haas, D. E.; Birnie, D. P. Nondestructive Measurement of Striation Defect Spacing Using Laser Diffraction. *J. Mater. Res.* **2001**, *16*, 3355–3360.
14. Jukes, P. C.; Heriot, S. Y.; Sharp, J. S.; Jones, R. A. L. Time-Resolved Light Scattering Studies of Phase Separation in Thin Film Semiconducting Polymer Blends During Spin-Coating. *Macromolecules* **2005**, *38*, 2030–2032.

15. Birnie, D. P.; Manley, M. Combined Flow and Evaporation of Fluid on a Spinning Disk. *Phys. Fluids* **1997**, *9*, 870–875.
16. Horowitz, F.; Dawnay, E. J. C.; Fardad, M. A.; Green, M.; Yeatman, E. M. Towards Better Control of Sol-Gel Film Processing for Optical Device Applications. *J. Nonlinear Opt. Phys.* **1997**, *6*, 1–18.
17. Horowitz, F.; Yeatman, E.; Dawnay, E.; Fardad, A. Real-Time Optical Monitoring of Spin-Coating. *J. Phys. III* **1993**, *3*, 2059–2063.
18. DalnokiVeress, K.; Forrest, J. A.; Stevens, J. R.; Dutcher, J. R. Phase Separation Morphology of Spin-Coated Polymer Blend Thin Films. *Physica A* **1997**, *239*, 87–94.
19. The scattering peak amplitude modulation results from the different heights between the two phases being a maxima when they are at $\Delta d = n(\lambda/6)$. In the case of this particular blend the final dry state approaches this, resulting in the large difference in intensities between the two domains. The short oscillations in the intensity for the 1d radially integrated data (freq = 0.16 s) are due to the different domains both generating equivalent reflection intensities and not due there being an actual lack of structure for these frames. This becomes apparent by consideration of the intensity curves for each domain (Figure 2a). Although out of phase, the lines cross at particular points in time, generating equal reflection intensities, giving the impression of a uniform film, with no structure or length scale present.
20. In some experiments, small contaminants present on the silicon surface acted as inadvertent tracer particles during the early stages of the spin-coating process and were shown to move under the radial centrifugal forces before becoming fixed within the film matrix. This shows the potential to use the stroboscopic methods to also investigate processes during the initial miscible phase regime.
21. Koyama, K.; Iwasaki, A.; Tanimoto, M.; Kudo, I. Simple Interferometric Microscopy for in Situ Real-Time Two-Dimensional Observation of Crystal Growth. *Rev. Sci. Instrum.* **1996**, *67*, 2584–2587.
22. To ensure accurate height reconstruction, the start time must be chosen in a position on the interference curve where the maxima and minima are prominent, to allow automated peak location by the analysis software across the entire image. In this case around 6 s of reconstruction was possible. Experimentally improving the incident light flux will allow longer reconstructions.
23. Liao, Y. G.; Su, Z. H.; Ye, X. G.; Li, Y. Q.; You, J. C.; Shi, T. F.; An, L. J. Kinetics of Surface Phase Separation for PMMA/SAN Thin Films Studied by In Situ Atomic Force Microscopy. *Macromolecules* **2005**, *38*, 211–215.